Direct Dynamics Study of the Hydrogen Abstraction Reaction of $CF_3CH_2Cl + Cl \rightarrow CF_3CHCl + HCl$

YUAN ZHAO,[1] HONGQING HE,[2] JINGLAI ZHANG,[1] LI WANG[1]

[1]*Institute of Environmental and Analytical Sciences, College of Chemistry and Chemical Engineering, Henan University, Kaifeng, Henan 475004, People's Republic of China*
[2]*Wuhan Center for Magnetic Resonance, State Key Laboratory of Magnetic Resonance and Atomic and Molecular Physics, Wuhan Institute of Physics and Mathematics, Chinese Academy of Sciences, Wuhan 430071, People's Republic of China*

Received 16 August 2010; revised 25 January 2011, 23 May 2011; accepted 28 November 2011

DOI 10.1002/kin.20709
Published online in Wiley Online Library (wileyonlinelibrary.com).

ABSTRACT: The hydrogen abstraction reaction of Cl atoms with CF_3CH_2Cl (HCFC-133a) is investigated by using density function theory and ab initio approach, and the rate constants are calculated by using the dual-level direct dynamics method. Optimized geometries and frequencies of reactants, transition state, and products are computed at the B3LYP/6-311+G(2d,2p) level. To refine the energetic information along the minimum energy path, single-point energy calculations are carried out at the G3(MP2) level of theory. The interpolated single-point energy method is employed to correct the energy profiles for the title reaction. The rate constants are evaluated by using the canonical variational transition state theory with a small-curvature tunneling correction over a wide range of temperature, 200–2000 K. The variational effect for the reaction is moderate at low temperatures and very small at high temperatures. However, the tunneling correction has an important contribution in the lower temperature

Correspondence to: L. Wang; e-mail: chemwangl@henu.edu.cn; J. Zhang; e-mail: zhangjinglai@henu.edu.cn.

Contract grant sponsor: National Natural Science Foundation of China.
Contract grant number: 21003036.
Contract grant sponsor: He'nan Educational Committee.
Contract grant numbers: 2008A150005, 2011B150003.
Contract grant sponsor: Science Foundation of Henan University.
Contract grant numbers: 2009YBZR013, SBGJ090507.
Contract grant sponsor: Doctor Foundation of Henan University.
Supporting information is available in the online issue at www.wileyonlinelibrary.com.

range. The agreement between calculated rate constants and available experimental values is good at lower temperatures but diverges significantly at higher temperatures. © 2012 Wiley Periodicals, Inc. Int J Chem Kinet 1–7, 2012

INTRODUCTION

The adverse effect of chlorofluorocarbons (CFCs) released into the atmosphere has led to an international focus on replacing CFCs with environment-friendly alternatives [1–3]. Hydrochlorofluorocarbons (HCFCs) are considered as the principal CFCs alternatives, which have been used in lubricants, solvents, refrigerants, and other applications. Incineration is thought to be an effective method for disposal of HCFCs. To incinerate industrial waste HCFCs in a more efficient and less hazardous way, it is essential to elucidate all aspects of this kind of combustion process. To understand the incineration mechanism and rate constants for important elementary reactions is necessary. Many kinetic studies have been carried out to determine the rates and mechanisms of these reactions.

In this paper, we focus our attention on the reaction of CF_3CH_2Cl with chlorine atoms. The rate constant of $CF_3CH_2Cl + Cl \rightarrow CF_3CHCl + HCl$ was previously measured at the temperature range of 298–500 [4] and 200–300 K [5,6], respectively. The corresponding Arrhenius expressions (in cm^3 $molecule^{-1}$ s^{-1}) 1.83×10^{-12} exp $[-(1710 \pm 257)/T]$ (298–500 K) and 1.80×10^{-12} exp $[-(1710 \pm 500)/T]$ (200–300 K) were reported by Jourdain et al. [4] and DeMore et al. [5,6], respectively. These two expressions exhibit good consistency. However, these results are slightly lower than those obtained by Møgelberg et al. [7] at 296 K. To the best of our knowledge, little theoretical attention has been paid to the title reaction.

Here, we employ the dual-level (X//Y) direct dynamics method proposed by Truhlar and coworkers [8–10] to study the kinetic nature of the title reaction. With this approach, we obtained the potential energy surface (PES) information directly from density function theory (DFT) calculations and evaluated the rate constants by using the variational transition-state theory (VTST) [11–13]. A comparison between theoretical and experimental results is discussed. We hope that the present theoretical studies are helpful in estimating the dynamics properties of the reaction over an appropriate temperature range.

CALCULATION METHODS

The equilibrium geometries and frequencies of all the stationary points (reactants, products, and transition state) included in the title reaction are optimized at two levels, i.e., Becke's three-parameter nonlocal-exchange functional with the nonlocal correlation functional of Lee–Yang–Parr (B3LYP) [14,15] with the 6-311+G(2d,2p) basis set [B3LYP/6-311+G(2d,2p)] and restricted or unrestricted second-order Møller–Plesset perturbation theory (MP2) with the 6-311G(d,p) basis set [MP2/6-311G(d,p)]. The minimum energy path (MEP) is obtained using the intrinsic reaction coordinate (IRC) theory to confirm that the transition state (TS) really connects the corresponding reactants and products along the reaction path. The first and second energy derivatives at geometries along the MEP are obtained to calculate the curvature of the reaction path and to calculate the generalized vibrational frequencies along the reaction path. To obtain a more trustworthy reaction enthalpy and barrier height, single-point corrections were performed by using G3(MP2) theory [16]. It should be noted that the G3(MP2) energies are obtained according the following equation: E[G3(MP2)] $= E$[QCISD(T)/6-31G(d)] $+ E$(MP2/G3MP2Large) $- E$[MP2/6-31G(d)] $+ \Delta E$(SO) $+ E$(HLC). Here, the single-point energy calculations are based on the B3LYP/6-311+G(2d,2p) and MP2/6-311G(d,p) optimized geometries, respectively. It has been shown that in many studies [17–21] this method can provide reliable PES information. Original G3(MP2) calculations are also performed for comparison. The dual-level potential profile along the reaction path is further refined with the interpolated single-point energies (ISPE) method [22], in which extra single-point calculations are employed to correct the lower level reaction path. All electronic structure calculations are carried out with the Gaussian 03 program package (Wallingford, CT) [23].

Rate constants were calculated using VTST proposed by Truhlar and coworkers. The specific level of VTST that we utilized is the conventional transition state theory (TST) and canonical variational transition state theory (CVT) [24], and the tunneling correction is considered by the centrifugal-dominant small-curvature semiclassical adiabatic ground-state (CD-SCSAG) [25,26] method, which is computed with equal segments in the Boltzmann and θ integrals, and the number of Gauss–Legendre quadrature points is chosen as 40 for computing the Boltzmann average. Also, the sixth-order Lagrangian interpolation is used to obtain the values of the effective mass for the

CD-SCSAG tunneling calculation. For the title reaction, two models are employed to treat the vibrations and the rate constants are calculated on the basis of two models (Models 1 and 2) for comparison. In Model 1 all vibrations are treated in the harmonic oscillator approximation and in Model 2 the lowest vibrational mode is treated using the hindered rotor model [27], whereas all other vibrational modes are treated as separable harmonic oscillators. In addition, the $^2P_{3/2}$ and $^2P_{1/2}$ electronic states of chlorine atom, with 881 cm^{-1} splitting due to the spin-orbit coupling, are included in the calculation of the electronic partition functions. The curvature components are computed by using a quadratic fit to obtain the derivative of the gradient with respect to the reaction coordinate. The rate constants calculations were performed by using the POLYRATE 9.7 program [28].

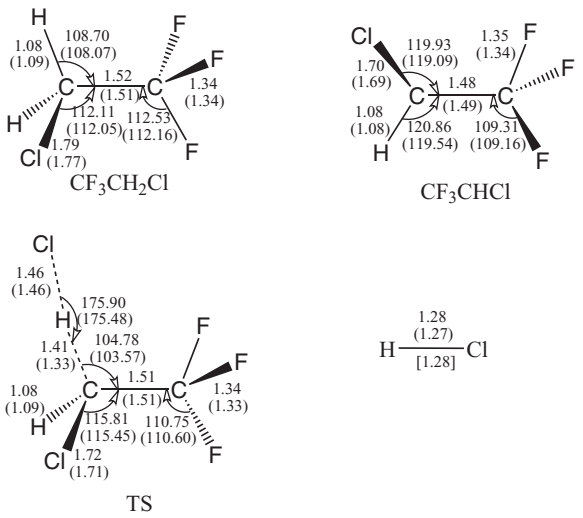

Figure 1 Optimized geometries of reactants, products, and TS at the B3LYP/6-311+G(2d,2p) level. The values in the parentheses are the values obtained at the MP2/6-311G(d,p) level. The value in the square brackets is the experimental value [29]. Bond lengths are in angstroms and angles are in degrees.

RESULTS AND DISCUSSION

Stationary Points

The geometric parameters of all the stationary points (reactants, products, and transition state) optimized at the B3LYP/6-311+G(2d,2p) and MP2/6-311G(d,p) levels are drawn in Fig. 1 along with the available experimental data [29]. The Cartesian coordinates and electronic energies for B3LYP/6-311+G(2d,2p) and MP2/6-311G(d,p) optimized geometries of all stationary points are listed in Tables S1 and S2 in the Supporting Information, respectively. It can be seen that the bond length of HCl calculated at the B3LYP and MP2 levels shows a good mutual agreement with the deviation of 0.01 Å. Both theoretical values also agree well with the corresponding experimental value (1.28 Å). At the B3LYP level, the breaking C—H bond is stretched by 30.6% in TS compared to the C—H equilibrium bond length in CF_3CH_2Cl. The forming H—Cl bond is elongated by 14.1% with respect to the equilibrium bond length in an isolated molecule HCl. The elongation of the breaking bond is greater than that of the forming bond, indicating that TS is product-like, i.e., the reaction will proceed via late TS.

Harmonic vibrational frequencies are calculated at the same level of theory to characterize the nature of each critical point and to make zero-point energy (ZPE) corrections. As shown in Table I, the calculated HCl frequency agrees well with the experimental value [30] with the relative error of 2.4% and 3.1% at the B3LYP and MP2 levels, respectively. All the reactants and products have real frequencies. TS is confirmed by using normal-mode analysis to have only one imaginary frequency, which has the values of 1088i and 1411i at the B3LYP and MP2 levels, respectively. In addition, the $\langle S^2 \rangle$ values are also listed in Table I. The $\langle S^2 \rangle$ values for the doublet before spin annihilation are almost equal to 0.75 at the B3LYP/6311+G(2d,2p) level. The corresponding value obtained at the MP2/6-311G(d,p) level is higher than the B3LYP result.

The reaction energy at 298 K (ΔH^0_{298}), the reaction energy at 0 K (ΔE), and barrier height (ΔV) calculated at the B3LYP/6-311+G(2d,2p), MP2/6-311G(d,p), G3(MP2)//B3LYP/6-311+G(2d,2p), and G3(MP2)//MP2/6-311G(d,p) levels, as well as the "experimental enthalpy," are summarized in Table II. It should be noted that the enthalpies of formation of CF_3CH_2Cl and CF_3CHCl are not experimental values, but were estimated with the use of isodesmic reactions [17]. Here, the average calculated enthalpies of formation (CF_3CH_2Cl, −179.76 ± 2.0 kcal mol^{-1}; CF_3CHCl, −131.93 ± 4.7 kcal mol^{-1}) [17] and experimental values of other two species (Cl, 29.01 kcal mol^{-1}; HCl, −22.07 kcal mol^{-1}) [31] are used together to calculate the "experimental enthalpy." For purposes of comparison, we also performed standard G3(MP2) calculations. The corresponding values are also listed in Table II. The values obtained at the higher levels, i.e., G3(MP2)//B3LYP/6-311+G(2d,2p), G3(MP2)//MP2/6-311G(d,p), and G3(MP2) levels, agree well with the "experimental ones." Moreover, the reaction enthalpy and barrier

Table I Calculated and Experimental Frequencies in cm^{-1} of the Reactants, Products, and TS at the B3LYP/6-311+G(2d,2p) Leve1

Species	Frequencies	Experimental[a]	$\langle S^2 \rangle$
HCl	2920 (3085)	2991	0.0
CF_3CH_2Cl	96 (108), 216 (193),346 (358), 403 (367), 522 (543), 538 (547), 653 (652), 833 (830), 966 (890), 1089 (940), 1144 (1169), 1180 (1203), 1285 (1321), 1300 (1342), 1433 (1412), 1491 (1485), 3080 (3153), 3138 (3227)		0.0
CF_3CHCl	34 (71), 182 (187), 214 (299), 363 (376), 401 (453), 528 (549), 557 (591), 644 (667), 817 (849), 932 (978), 1086 (1187), 1119 (1204), 1230 (1303), 1349 (1417), 3256 (3304)		0.754
TS	1088*i* (1411i), 48 (55), 73 (74), 131 (135), 186 (194), 300 (306), 357 (371), 441 (442), 528 (545), 537 (556), 644 (667), 823 (853), 854 (901), 891 (952), 937 (1003), 1063 (1120), 1143 (1216), 1145 (1245), 1249 (1315), 1323 (1387), 3171 (3210)		0.756 (0.789)

The values in parentheses are the theoretical values obtained at the MP2/6-311G(d,p) level.
[a]From Ref. [30].

Table II Enthalpies and Barrier Heights at the B3LYP/6-311+G(2d,2p), MP2/6-311G(d,p), G3(MP2)//B3LYP/6-311+G(2d,2p), G3(MP2)//MP2/6-311G(d,p), and G3(MP2) Levels Along with Available Experimental Value

	ΔH^0_{298}(kcal mol^{-1})	ΔE(0 K)	ΔV (kcal mol^{-1})
B3LYP/6-311+G(2d,2p)	−5.02	−5.90	0.28
MP2/6-311G(d,p)	0.94	0.17	7.92
G3(MP2)//B3LYP/6-311+G(2d,2p)	−3.83	−4.72	3.03
G3(MP2)//MP2/6-311G(d,p)	−3.61	−4.38	3.41
G3(MP2)	−4.14	−4.35	3.24
Experimental[a]	-3.25 ± 6.7		

[a]From Refs. [17,31].

height calculated at the three higher levels agree within 0.6 kcal mol^{-1}. Since the MP2 method is very expensive, the less expensive B3LYP method, which also has fewer problems with spin contamination, was employed to calculate the energies.

The MEP is calculated by using the IRC theory at the B3LYP/6-311+G(2d,2p) level, and the kinetic calculations of the title reaction are carried out using the VTST with the ISPE (VTST–ISPE) method at the G3(MP2)//B3LYP level. The classical potential energy [$V_{MEP}(s)$], the ground-state vibrational adiabatic potential energy [$V_a^G(s)$], and the ZPE curves of reaction as functions of IRC (s) are plotted in Fig. 2, where the ground-state vibrationally adiabatic potential curve is defined as $V_a^G(s) = V_{MEP}(s) + \mathrm{ZPE}(s)$. Note that the maximum of the potential energy profile at the G3(MP2)//B3LYP level is slightly shifted in the s direction in Fig. 2. This is the case that the saddle point position of the dual level is generally shifted with the VTST–ISPE scheme [22].

KINETICS CALCULATIONS

The dual-level (X//Y) direct dynamics calculations are carried out for the title reaction by using the VTST–ISPE approach [22]. The PES information for the reaction obtained at the G3(MP2)//B3LYP level is put into POLYRATE 9.7 program to calculate the VTST rate constants over the temperature range from 200 to 2000 K. The forward rate constants are calculated by using the conventional transition-state theory (TST), CVT, and CVT with the small-curvature tunneling (SCT) correction.

The TST, CVT, and CVT/SCT rate constants calculated with the use of Model 1 are shown in Fig. 3. It is found that the TST rate constants are slightly more than CVT rate constants at low temperatures, whereas the differences between TST and CVT ones become smaller with increasing temperature. The ratios of k_{TST}/k_{CVT} are 1.89 at 200 K, 1.37 at 300 K, and 1.19 at 2000 K. On the other hand, the CVT/SCT rate constants are greater than the CVT ones below 400 K.

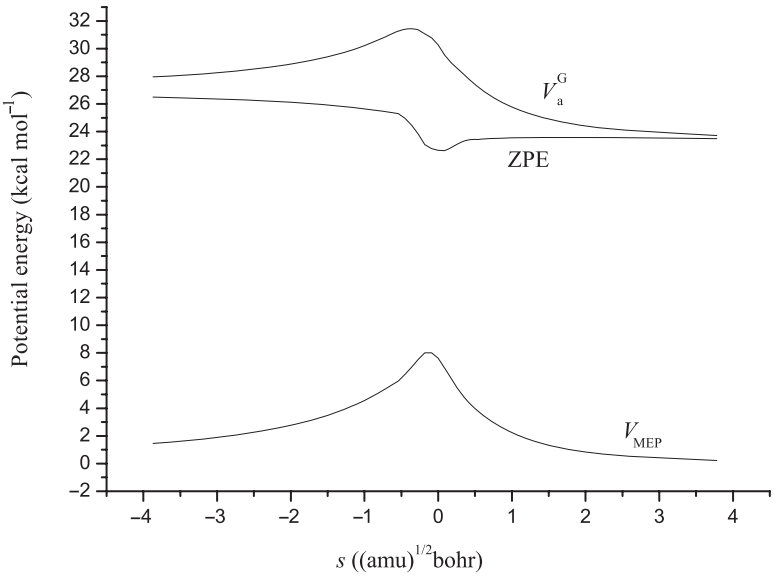

Figure 2 Classical potential energy curve (V_{MEP}), ground-state vibrationally adiabatic energy curve (V_a^G), and zero-point-energy curve ZPE as functions of s(amu)$^{1/2}$ bohr at the G3(MP2)//B3LYP/6-311+G(2d,2p) level for the reaction $CF_3CH_2Cl + Cl \rightarrow CF_3CHCl + HCl$.

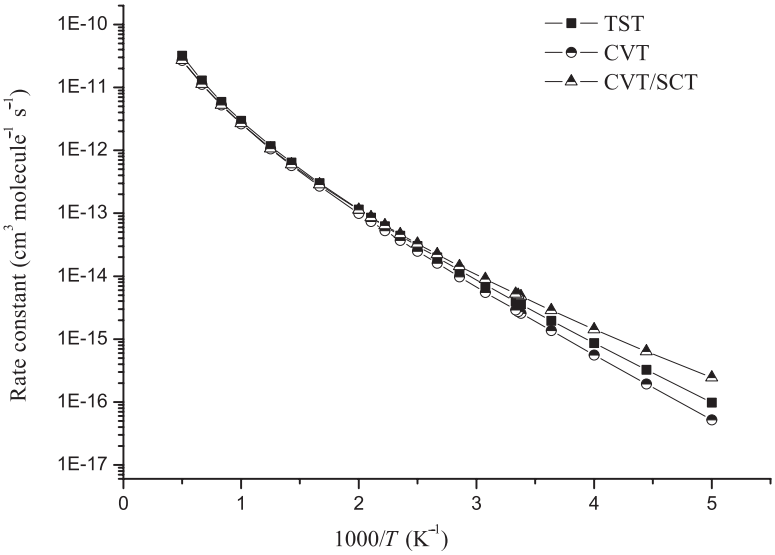

Figure 3 Plot of the TST, CVT, and CVT/SCT rate constants calculated at the G3(MP2)//B3LYP/6-311+G(2d,2p) level by using the Model 1 versus 1000/T between 200 and 2000 K for the reaction $CF_3CH_2Cl + Cl \rightarrow CF_3CHCl + HCl$.

For example, the ratios of $k_{CVT/SCT}/k_{CVT}$ are 4.73, 1.81, and 1.31 at 200, 300, and 400 K, respectively. Thus, the small curvature correction plays an important role at the low temperatures. A similar conclusion can be drawn from the results calculated by using Model 2.

The CVT/SCT rate constants calculated with the use of two models are labeled as k_{m1} and k_{m2}, respectively. The temperature dependence of the rate constants and available experimental values are presented in Fig. 4. As shown in Fig. 4, k_{m1} and k_{m2} are in much better accord with the experimental values at the temperature range of 200–300 K [5,6] and 296 K [7]. The deviation factors of $k_{m1}/k_{expt.}$ and $k_{m2}/k_{expt.}$ are 0.7–0.9 and 0.9–1.2, respectively. However, both k_{m1} and k_{m2} diverge significantly from the experimental values at higher temperatures. The divergence may be caused by the incorrect treatment for the torsions. The reaction $CF_3CH_2Cl + Cl$ has torsions at reactant and saddle point. Thus, the lowest vibrational mode should be treated using the internal rotor

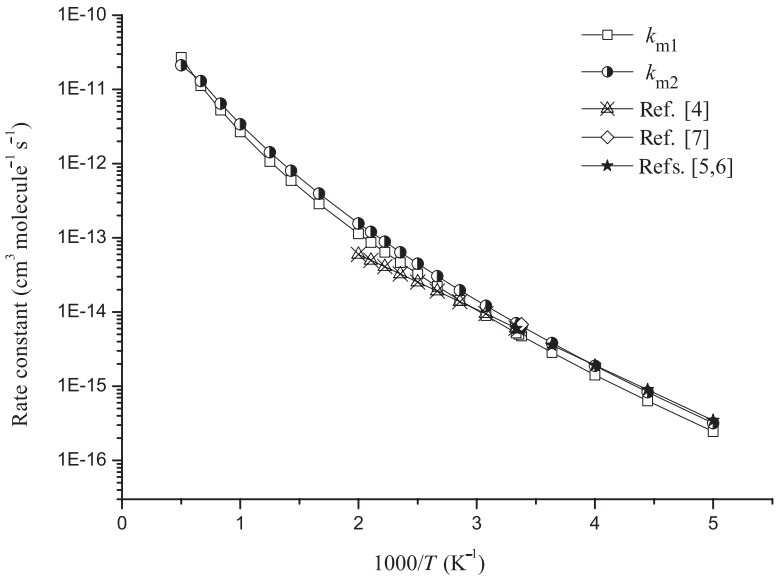

Figure 4 Plot of CVT/SCT rate constants calculated at the G3(MP2)//B3LYP/6-311+G(2d,2p) level with the use of Models 1 and 2 along with the available experimental values versus 1000/T between 200 and 2000 K for the reaction $CF_3CH_2Cl + Cl \rightarrow CF_3CHCl + HCl$.

model [27]. But all of them are complicated motions involving more than one torsion or mixtures of torsion and bending. Neither the internal rotor model nor the harmonic oscillator approximation is exactly correct to describe the complicated motion [32]. We hope that new model can be developed further to solve this problem.

Although there is a deviation between theoretical and some experimental rate constants, the three-parameter fits for the CVT/SCT rate constants between 200 and 2000 K, (in units of cm^3 molecule^{-1} s^{-1}) $k_{m1} = 9.43 \times 10^{-20}\ T^{2.66} \exp(-1261.9/T)$ and $k_{m2} = 4.76 \times 10^{-18}\ T^{2.14} \exp(-1465.6/T)$, are presented for convenience of future experimental measurements.

CONCLUSIONS

In this paper, the hydrogen abstraction reaction of CF_3CH_2Cl with Cl atoms is investigated by using the dual-level direct dynamics method. Dynamics calculation are carried out by using the VTST–ISPE method at the G3(MP2)//B3LYP/6-311+G(2d,2p) level. The harmonic oscillator model and internal rotor model are employed to treat the vibrations, respectively. The rate constants calculated by using the CVT with a small-curvature tunneling correction (SCT) agree well with the experimental values at lower temperatures but diverge significantly at higher temperatures. The three-parameter expressions (in cm^3 molecule $^{-1}$ s^{-1}) for the reaction in the temperature range of 200–2000 K are $k_{m1} = 9.43 \times 10^{-20}\ T^{2.66} \exp(-1261.9/T)$ and $k_{m2} = 4.76 \times 10^{-18}\ T^{2.14} \exp(-1465.6/T)$. We hope that more experiments are to be performed to verify the current results, especially at higher temperatures.

We thank Professor Donald G. Truhlar for providing the POLYRATE 9.7 program and the state key laboratory of physical chemistry of solid surfaces for providing computational resources.

BIBLIOGRAPHY

1. Talhaoui, A.; Louis, F.; Devolder, P.; Meriaux, B.; Sawerysyn, J. P. J Phys Chem 1996, 100, 13531–13538.
2. Liu, R.; Huie, R. E.; Kurylo, M. J. J Phys Chem 1990, 94, 3247–3249.
3. Hsu, K. J.; DeMore, W. B. J Phys Chem 1995, 99, 1235–1244.
4. Jourdain, J. L.; Le Bras, G.; Combourieu, J. J Chim Phys 1978, 75, 318–323.
5. DeMore, W. B.; Sander, S. P.; Golden, D. M.; Hampson, R. F.; Kurylo, M. J.; Howard, C. J.; Ravishankara, A. R.; Kolb, C. J.; Molina, M. J. Chemical Kinetics and Photochemical Data for Use in Stratospheric Modeling Evaluation Number 11, JPL Publication 94-26, 1994.
6. DeMore, W. B.; Sander, S. P.; Golden, D. M.; Hampson, R. F.; Kurylo, M. J.; Howard, C. J.; Ravishankara, A. R.; Kolb, C. J.; Molina, M. J. Chemical Kinetics and

Photochemical Data for Use in Stratospheric Modeling Evaluation Number 12, JPL Publication 97-4, 1997.
7. Møgelberg, T. E.; Nielsen, O. J.; Sehested, J.; Wallington, T. J. J Phys Chem 1995, 99, 13437–13444.
8. Truhlar, D. G. In The Reaction Path in Chemistry: Current Approaches and Perspectives; Heidrich, D., Ed.; Kluwer: Dordrecht, The Netherlands, 1995; p. 229.
9. Hu, W. P.; Truhlar, D. G. J Am Chem Soc 1996, 118, 860–869.
10. Truhlar, D. G.; Garrett, B. C.; Klippenstein, S. J. J Phys Chem 1996, 100, 12771–12800.
11. Truhlar, D. G.; Garrett, B. C. Acc Chem Res 1980, 13, 440–448.
12. Truhlar, D. G.; Isaacson, A. D.; Garrett, B. C. In The Theory of Chemical Reaction Dynamics; Baer, M., Ed.; CRC Press:, Boca Raton, FL, 1985; p. 65.
13. Truhlar, D. G.; Garrett, B. C. Annu Rev Phys Chem 1984, 35, 159–189.
14. Becke, A. D. J Chem Phys 1993, 98, 1372–1377.
15. Lee, C.; Yang, W.; Parr, R. G. Phys Rev B 1998, 37, 785–789.
16. Curtiss, L. A.; Redfern, P. C.; Raghavachari, K.; Rassolov, V.; Pople, J. A. J Chem Phys 1999, 110, 4703–4709.
17. Wang, L.; Zhao, Y.; Zhang, J.; Dai, Y. N.; Zhang, J. L. Theor Chem Acc 2011, 128, 183–189.
18. Wang, L.; Zhao, Y.; Wang, Z. Q.; Ju, C. G.; Feng, Y. L.; Zhang, J. L. J Mol Struct-Theochem 2010, 959, 101–105.
19. Yang, L.; Liu, J. Y.; Wan, S. Q.; Li, Z. S. J Comput Chem 2009, 30, 565–580.
20. Liu, H.X.; Wang, Y.; Yang, L.; Liu, J. Y.; Gao, H.; Li, Z. S.; Sun, C. C. J Comput Chem 2009, 30, 2194–2204.
21. Yang, L.; Liu, J. Y.; Wang, L.; He, H. Q.; Wang, Y.; Li, Z. S.; Sun, C. C. J Comput Chem 2008, 29, 550–561.
22. Chuang, Y. Y.; Corchado, J. C.; Truhlar, D. G. J Phys Chem 1999, 103, 1140–1149.
23. Frisch, M. J.; Trucks, G. W.; Schlegel, H. B.; Scuseria, G. E.; Rob, M. A.; Cheeseman, J. R.; Montgomery, J. A., Jr; Vreven, T.; Kudin, K. N.; Burant, J. C.; Millam, J. M.; Iyengar, S. S.; Tomasi, J.; Barone, V.; Mennucci, B.; Cossi, M., Scalmani, G.; Rega, N.; Petersson, G. A.; Nakatsuji, H.; Hada, M.; Ehara, M.;Toyota, K.; Fukuda, R.; Hasegawa, J.; Ishida, M.; Nakajima, T.; Honda, Y.; Kitao, O.; Nakai, H.; Klene, M.; Li, X.; Knox, J. E.; Hratchian, H. P.; Cross, J. B.; Bakken, V.; Adamo, C.; Jaramillo, J.; Gomperts, R.; Stratmann, R. E.; Yazyev, O.; Austin, A. J.; Cammi, R.; Pomelli, C.; Ochterski, J. W.; Ayala, P. Y.; Morokuma, K.; Voth, G. A.; Salvador, P.; Dannenberg, J. J.; Zakrzewski, V. G.; Dapprich, S.; Daniels, A. D.; Strain, M. C.; Farkas, O.; Malick, D. K.; Rabuck, A. D.; Raghavachari, K.; Foresman, J. B.; Ortiz, J. V.; Cui, Q.; Baboul, A. G.; Clifford, S.; Cioslowski, J.; Stefanov, B. B.; Liu, G.; Liashenko, A.; Piskorz, P.; Komaromi, I.; Martin, R. L.; Fox, D. J.; Keith, T.; Al-Laham, M. A.; Peng, C. Y.; Nanayakkara, A.; Challacombe, M.; Gill, P. M. W.; Johnson, B.; Chen, W.; Wong, M. W.; Gonzalez, C.; Pople, J. A. Gaussian 03 2003, Gaussian, Inc., Pittsburgh, PA.
24. Garrett, B. C.; Truhlar, D. G. J Chem Phys 1979, 70, 1593–1598.
25. Lu, D. H.; Truong, T. N.; Melissas, V. S.; Lynch, G. C.; Liu, Y. P.; Grarrett, B. C.; Steckler, R.; Issacson, A. D.; Rai, S. N.; Hancock, G. C.; Lauderdale, J. G.; Joseph, T.; Truhlar, D. G. Comput Phys Commun 1992, 71, 235–263.
26. Liu, Y. P.; Lynch, G. C.; Truong, Y. N.; Lu, D.; Truhlar, D. G.; Garrett, B. C. J Am Chem Soc 1993, 115, 2408–2415.
27. Chuang, Y. Y.; Truhlar, D. G. J Chem Phys 2000, 112, 1221–1228.
28. Corchado, J. C.; Chuang, Y. Y.; Fast, P. L.; Hu, W. P.; Liu, Y.-P.; Lynch, G. C.; Nguyen, K. A.; Jackels, C. F.; Fernandez-Ramos, A.; Ellingson, B. A.; Lynch, B. J.; Zheng, J. J.; Melissas, V. S.; Villa, J.; Rossi, I.; Coitino, E. L.; Pu, J. Z.; Albu, T. V.; Steckler, R.; Garrett, B. C.; Isaacson, A. D.; Truhlar, D. G. POLYRATE, version 9.7; University of Minnesota: Minneapolis, MN, 2007.
29. Huber, K. P.; Herzberg, G. Molecular Spectra and Molecular Structure IV. Constants of Diatomic Molecules; Van Nostrand-Reinhold: New York, 1979.
30. Stull, D. R.; Prophet, H. JANAF Thermochemical Tables, 2nd ed.; National Standard Reference Data Series; National Bureau of Standards: Washington, DC, 1971; Vol. 37, pp. 1971.
31. Chase, M. W., Jr. NIST–JANAF Themochemical Tables, 4th ed.,J. Phys Chem Ref Data 9 1998, 1–1951.
32. Zheng, J. J.; Truhlar, D. G. Phys Chem Chem Phys 2010, 12, 7782–7793.